THE UNIVERSITY OF
WARWICK

Author(s): C. Tappert, L. Schmidtobreick, R. E. Mennickent, F. P.
Navarrete, B. T. Gänsicke
Article Title: K-band spectroscopy of pre-cataclysmic variables
Year of publication: 2007
Link to published article:
http://dx.doi.org/10.1051/0004-6361:20077679
Publisher statement: © ESO 2007. Tappert, C. et al. (2007). K-band
spectroscopy of pre-cataclysmic variables. Astronomy & Astrophysics,
Vol.475(2), pp.575-583

Astronomy & Astrophysics

K-band spectroscopy of pre-cataclysmic variables[⋆]

C. Tappert[1], B. T. Gänsicke[2], L. Schmidtobreick[3], R. E. Mennickent[4], and F. P. Navarrete[1]

[1] Departamento de Astronomía y Astrofísica, Pontificia Universidad Católica, Vicuña Mackenna 4860, 782-0436 Macul, Chile
    e-mail: ctappert@astro.puc.cl, fpnavarr@puc.cl
[2] Department of Physics, University of Warwick, Coventry CV4 7AL, UK
    e-mail: Boris.Gaensicke@warwick.ac.uk
[3] European Southern Observatory, Casilla 19001, Santiago 19, Chile
    e-mail: lschmidt@eso.org
[4] Departamento de Física, Universidad de Concepción, Casilla 160-C, Concepción, Chile
    e-mail: rmennick@astro-udec.cl

ABSTRACT

Aims. There exists now substantial evidence for abundance anomalies in a number of cataclysmic variables (CVs), indicating that the photosphere of the secondary star incorporates thermonuclear processed material. However, the spectral energy distribution in CVs is usually dominated by the radiation produced by the accretion process, severely hindering an investigation of the stellar components. On the other hand, depending on how the secondary star has acquired such material, the above mentioned abundance anomalies could also be present in pre-CVs, i.e. detached white/red dwarf binaries that will eventually evolve into CVs, but have not yet started mass transfer, and therefore allow for an unobstructed view on the secondary star at infrared wavelengths.
Methods. We have taken *K*-band spectroscopy of a sample of 13 pre-CVs in order to examine them for anomalous chemical abundances. In particular, we study the strength of the ^{12}CO and ^{13}CO absorption bands that have been found diminished and enhanced, respectively, in similar studies of CVs.
Results. All our systems show CO abundances that are within the range observed for single stars. The weakest ^{12}CO bands with respect to the spectral type are found in the pre-CV BPM 71214, although on a much smaller scale than observed in CVs. Furthermore there is no evidence for enhanced ^{13}CO. Taking into account that our sample is subject to the present observational bias that favours the discovery of young pre-CVs with secondary stars of late spectral types, we can conclude the following: 1) our study provides observational proof that the CO anomalies discovered in certain CVs are not due to any material acquired during the common envelope phase, and 2) if the CO anomalies in certain CVs are not due to accretion of processed material during nova outburst, then the progenitors of these CVs are of a significantly different type than the currently known sample of pre-CVs.

Key words. stars: binaries: close – stars: late-type – stars: novae, cataclysmic variables – infrared: stars

1. Introduction

A cataclysmic variable (CV) is a close interacting binary consisting of a white dwarf (WD) and a red (K–M) main-sequence star (RD). The latter, secondary star, transfers mass via Roche-lobe overflow to the more massive white dwarf, the primary component. Typical orbital periods range from ~80 min to ~10 h. For comprehensive overviews on CVs see Warner (1995) and Hellier (2001).

The progenitors of CVs are thought to be initially wide, detached binaries. As the more massive component expands in the course of its nuclear evolution, it fills its Roche lobe and transfers matter at high rates onto the red dwarf. At mass-loss rates $\dot{M}_1 \sim 0.1\ M_\odot\ \mathrm{yr}^{-1}$, the corresponding dynamical time scale is much shorter than the Kelvin-Helmholtz time scale for thermal adjustment of the secondary star. A common-envelope (CE) configuration results, providing an enhanced braking mechanism that rapidly shrinks the orbital separation, until, at $P_{\mathrm{orb}} \lesssim 1$ d, the kinetic energy stored in the CE exceeds the binding energy, and the CE is expelled as a planetary nebula, leaving a close, but still detached, WD/RD binary. The remaining mechanisms for angular-momentum loss, magnetic braking and/or gravitational radiation, further shrink the orbital separation, now

on a much longer time scale, until the Roche lobe of the secondary star comes into contact with the stellar surface, initiating mass-transfer and the proper CV phase. Systems that have gone through such a CE configuration and eventually will evolve into a CV, are known as post-CE binaries. Using the criterion by Schreiber & Gänsicke (2003), such objects are called pre-CVs if they evolve into CVs in less than Hubble time (~13 Gyr) and can thus be regarded as representative progenitors of the current CV population.

While it had been originally assumed that the secondaries enter the CV phase as main-sequence stars, during the past decade substantial evidence has been amounted that a large fraction of the secondary stars in long-period ($P_{\mathrm{orb}} > 3$ h) CVs shows signs of nuclear evolution (Beuermann et al. 1998; Harrison et al. 2004, 2005b). This would mean that the binary spends a much longer time in its pre-CV state than hitherto assumed, and could provide the solution to certain discrepancies between modelled and observed CV population (e.g. Patterson 1998; Gänsicke 2005).

In particular, the work by Harrison et al. revealed diminished ^{12}CO and – in comparison – enhanced ^{13}CO absorption bands in the *K* spectra of dwarf novae with orbital periods >3 h, which they interpret as being due to CNO processed material finding its way into the stellar photosphere of the secondary star. Currently discussed scenarios that could lead to this

phenomenon can be divided in two principal categories: 1) nuclear evolution of the secondary star, and 2) accretion of nuclear processed material.

The former implies that sufficient time for nuclear evolution has to pass from the CE to the CV phase, and is only feasible for secondary stars of comparatively early spectral type ($\lesssim$K0V) since dwarfs of later spectral type will not evolve within Hubble time (e.g. Pols et al. 1998). As a consequence, the secondary star temporarily might become the more massive component after the CE phase, and go through a phase of thermal-timescale mass transfer (Schenker & King 2002; Schenker et al. 2002; Gänsicke et al. 2003; Harrison et al. 2005a, the latter discuss this in the context of anomalous abundances).

For the accretion scenario there are two principle sources of processed material: either the secondary star swept up processed material during the CE phase, or it accreted ejected material during nova eruptions. These possibilities have been discussed by Marks & Sarna (1998), who find that the significance of such effect strongly depends on the (unknown) efficiency of the secondary to accrete such material. Furthermore, in the case of accretion from the CE, such material will be stripped away from the secondary already in the early stages of the semi-detached CV phase (see also the respective discussion in Harrison et al. 2004).

Both the evolution scenario and accretion from the CE would also lead to anomalous chemical abundances in the progenitors of CVs, i.e. in pre-CVs. We here present *K* band spectroscopy of a sample of pre-CVs to investigate the strength of the CO features in these systems.

2. The sample

We have used the TPP catalogue (Kube et al. 2002) to search for confirmed and candidate pre-CVs that are observable from the southern hemisphere. We have restricted our sample to confirmed pre-CVs with known orbital period, and excluded systems in nebulae and with primary components other than white dwarfs. There are a number of exceptions to the first criterion, in that we include three systems with uncertain orbital periods, and one, as yet unconfirmed pre-CV candidate P83l-57 (also known as Ret1; Downes et al. 2005). These objects have been part of a project that aimed at confirming the pre-CV nature of a number of candidates, and finding the orbital period by photometric means (Tappert et al. 2004, 2006b). The light curves of EC 12477-1738, EC 13349-3237, and EC 14329-1625, showed the periodic modulations that are typical for the sinusoidal or ellipsoidal variations in pre-CVs, although due to insufficient data no conclusive period could be determined. Initial observations of P83l-57 showed variations that could be interpreted as part of a pre-CV light curve: a decline of ~0.005 mag over ~5 h in one night, and a rise of similar dimensions in the subsequent night, and thus the object was included in our target list for the *K* band spectroscopy. However, later observations could not confirm this variation, so that the pre-CV status of P83l-57 remains doubtful at the moment and needs to be clarified by future observations.

Previous studies have already provided an estimate of the spectral type of the secondary star for about two thirds of the systems in our sample. All of them are M dwarfs that have time scales for nuclear evolution $>t_{Hubble} \sim$ 13 Gyr (e.g. Pols et al. 1998). Furthermore, most of these systems are relatively young objects, with white dwarf cooling times of less than a few 10^8 yr (except RR Cae and LTT560, which are ~1 Gyr old). Given that the typical time to evolve into a semidetached CV configuration

is several Gyr (assuming the standard prescription for orbital angular momentum loss, Schreiber & Gänsicke 2003), most of the systems have lived only through a relatively small fraction of their pre-CV live. In fact, only EC 13471-1258 and potentially BPM 71214 (depending on the model for angular momentum loss) have already passed more than half of their time as a post-CE binary. In this, our sample reflects the present observational bias towards systems with hot white dwarf primaries and/or comparatively late-type secondary stars (Schreiber & Gänsicke 2003). Our targets therefore do not represent the progenitors of CVs with anomalous abundances if scenario 1 (evolution) applies. A positive detection of anomalous CO strengths in our targets would be a strong indication that such material has been acquired by the secondary star during the CE phase (Marks & Sarna 1998).

For comparison we observed three late-type M dwarfs with spectral types similar to those of our program objects. Table 1 presents selected known properties of our targets.

3. Observations and data reduction

The data were obtained with ISAAC mounted at Antu (UT1), VLT, Paranal, Chile. The instrument was operated in SWS (short-wavelength spectroscopy) mode, and the grating was used in its low-resolution (resolving power ~1500), *K*-band, position. The nominal wavelength coverage was ~1.85–2.57 μ, though only data in the wavelength range ~2.00–2.45 μ were useful. Observations were conducted in service mode and included flat fields and wavelength calibration (Xe-Ar) data at the start of night, and telluric standard stars taken within 1 h and an airmass difference $\Delta M(z) = 0.2$ of the target spectra. The data were taken in AB–BA cycles, i.e. with small telescope offsets after the first and then after every second spectrum, so that spectra 1, 4, 5, 8, ..., occupy positions in the lower half of the CCD (position A), and spectra 2, 3, 6, 7, ..., are located in the upper half of the CCD (position B). Some stars were observed twice, since the first observations did not match ESO's quality criteria (regarding, e.g., seeing, difference in airmass between target and telluric standard, etc.). In one case (CC Cet), both spectra were found to be of sufficient quality, and could be combined in order to improve the S/N. For another system (BPM 6502) the spectra of the telluric standards presented significant disturbances on both occasions, fortunately once affecting mostly the blue part, and the other time mostly the red part of the spectrum. The latter spectrum was used for the SED analysis, since the spectral slope remained mostly intact. On the other hand, in the former spectrum, the spectral lines were not affected, and so this spectrum was used to measure equivalent widths. In the cases of P83l-57 and RE1016-053, only the second epoch data were useful. Table 2 presents a summary of the observations.

The reduction was done with IRAF packages. After flatfielding, a two-dimensional wavelength calibration was applied to the object data, in order to correct for the positional dependence of the dispersion. The resulting, "straightened", AB pairs of a specific object were then subtracted from each other and, after corresponding offsets had been applied, combined to a single image. Subsequently, the spectra of the targets and the telluric standards were extracted. For some days, no Xe-Ar wavelength calibration was provided. In these cases, it was found that calibration data from other days were sufficient to perform the 2-D transformation, but that it was necessary to apply a zero point correction to the extracted data using the night sky lines (Rousselot et al. 2000).

Table 1. Previously known properties of the sample stars. Coordinates (J2000.0) were taken from SIMBAD, JHK_s magnitudes are from the 2MASS database. Typical photometric errors are ~0.03 mag for K_s, and ~0.036 for the colours. Uncertain orbital periods are marked with a colon.

Name	RA	Dec	K_s	$J-H$	$H-K_s$	P_{orb} [h]	spType	References
BPM 6502	10 44 11	−69 18 20	10.56	0.527	0.335	8.08		Kawka et al. (2000)
BPM 71214	03 32 43	−08 55 40	9.30	0.655	0.233	4.33	M2.5V	Kawka et al. (2002)
CC Cet	03 10 55	+09 49 27	12.93	0.540	0.249	6.82	M4.5–M5V	Saffer et al. (1993)
EC 12477-1738	12 50 22	−17 54 46	12.60	0.639	0.262	13.7:		Tappert et al. (2004)
EC 13349-3237	13 37 51	−32 52 22	13.25	0.669	0.129	11.4:		Tappert et al. (2004)
EC 13471-1258	13 49 52	−13 13 38	9.98	0.558	0.288	3.62	M3.5–M4V	Kilkenny et al. (1997), O'Donoghue et al. (2003)
EC 14329-1625	14 35 46	−16 38 17	10.87	0.580	0.288	8.4:		Tappert et al. (2006b)
LTT 560	00 59 29	−26 31 01	11.86	0.521	0.270	3.54	M5.5V	Tappert et al. (2006a), Hoard & Wachter (1998)
NN Ser	15 52 56	+12 54 44	16.17	0.653	0.086	3.12	M4.75V	Haefner (1989), Haefner et al. (2004)
P83l-57	03 34 34	−64 00 56	11.54	0.594	0.204			
RE 1016-053	10 16 29	−05 20 27	9.77	0.617	0.220	18.9	M1.5V	Thorstensen et al. (1996)
RR Cae	04 21 06	−48 39 08	9.85	0.572	0.296	7.29	≳M6V	Bruch & Diaz (1998), Bruch (1999)
							M4V	Maxted et al. (2007)
UZ Sex	10 28 35	+00 00 29	10.94	0.532	0.276	14.3	M4V	Saffer et al. (1993)
1E 2310.4-4949	23 13 17	−49 33 16	8.92	0.623	0.219	–	M3Ve	Stocke et al. (1991)
J223315.83-603224.0	22 33 16	−60 32 24	10.74	0.660	0.155	–	M2V	Oliver et al. (2002)
LP 759-25	22 05 36	−11 04 29	10.72	0.607	0.329	–	M5.5V	Kirkpatrick et al. (1995)

Table 2. Log of observations, containing the date of the observations (start of night), the number of individual spectra, the exposure time for a single exposure, and the total exposure time. The last three columns give the corresponding atmospheric standard star, its spectral type, and its adopted effective temperature.

Object	Date	n_{data}	t_{exp} [s]	t_{tot} [s]	std	spType	T_{eff} [K]
BPM 6502	2005-12-21	2	10	20	Hip030743	B4V	17 000
	2006-01-12	2	10	20	Hip031068	B3V	19 000
BPM 71214	2005-11-17	2	5	10	Hip026939	B5V	15 200
CC Cet	2005-10-13	10	60	600	Hip024809	B9V	10 300
	2005-11-12	10	60	600	Hip034669	B4V	17 000
EC 12477-1738	2005-03-28	10	60	600	Hip065475	B2IVn	21 000
EC 13349-3237	2005-04-18	10	60	600	Hip055051	B1V	25 500
EC 13471-1258	2005-04-18	2	5	10	Hip055051	B1V	25 500
EC 14329-1625	2005-04-18	2	10	20	Hip055051	B1V	25 500
LTT 560	2005-06-01	2	30	60	Hip104320	B3V	19 000
NN Ser	2005-03-28	24	300	7200	Hip081362	B0.5III	27 750
P83l-57	2005-11-17	2	30	60	Hip026939	B5V	15 200
	2005-11-22	2	30	60	Hip015188	B3V	19 000
RE 1016-053	2005-12-24	2	5	10	Hip050780	B3V	19 000
	2006-01-12	2	5	10	Hip033575	B2V	21 000
RR Cae	2005-11-17	2	5	10	Hip026939	B5V	15 200
UZ Sex	2006-01-12	2	10	20	Hip033575	B2V	21 000
1E 2310.4-4949	2005-05-26	2	5	10	Hip088426	G0V	5940
J223315.83-603224.0	2005-05-25	2	10	20	Hip095103	G3V	5700
LP 759-25	2005-05-25	2	10	20	Hip105633	B2/B3V	20 200

With Brγ at 2.17 μ, the telluric standards of spectral type B have basically only one intrinsic absorption line in the *K* band. The very early type B stars also show a very weak HeI line at 2.11 μ. In both cases, those lines were fitted with a Voigt profile and subsequently subtracted from the spectrum. For the standards of spectral type G, a solar spectrum (NSO/Kitt Peak FTS data) was rebinned and smoothed down to the resolution of the ISAAC spectra, shifted in wavelength to correct for different zero points, and finally subtracted from the telluric spectra. The resulting pure atmospheric absorption spectra were then shifted and scaled to match position and depth of the atmospheric features in the corresponding target spectrum. Reference points for the shifting were the narrow absorption lines in the red part of the spectrum, while the broad feature between 2.0 and 2.1 μ was used to adjust for the depth of the atmospheric absorption. Finally, the target spectra were divided by the telluric spectra,

and, in order to recover the intrinsic SED of the targets, multiplied with a blackbody spectrum corresponding to the effective temperature of the telluric standard (see Table 2).

4. Results

4.1. Spectral types

Based on optical spectra, earlier studies have provided estimates of the spectral type for the majority of the targets in our sample. To obtain independent estimates for the spectral types of the secondary stars in our program pre-CVs, we have compared our *K* spectra to the spectral catalogues of Leggett et al. (2000), Kleinmann & Hall (1986), and Ivanov et al. (2004)[1] (hereafter

---

[1] See http://ftp.jach.hawaii.edu/ukirt/skl/dM.spectra/ for Leggett's data, the other two are available via CDS.
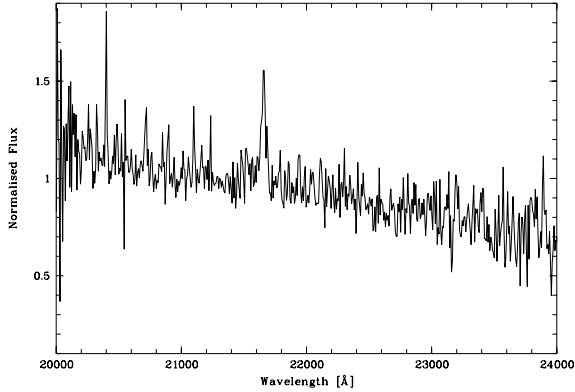
Fig. 1. Unsmoothed *K*-band spectrum of NN Ser. The only detected spectral feature is the Brγ emission line.

L00, KH86, and I04, respectively). Each catalogue has strengths and weaknesses for this application. The L00 data represent the best coverage of spectral subtypes, but are limited to M dwarfs, and have very low spectral resolution. The I04 catalogue still provides a very acceptable number of K and M dwarfs, at an only slightly lower spectral resolution than our data. However, their spectra are normalised with respect to the continuum slope, and thus there is no information on the SED. Finally, the KH86 sample contains only 4 late-type dwarfs, but provides the highest spectral resolution, and, although the library data are continuum normalised, the SED can be recovered by multiplying the spectra with the blackbody spectrum of an A0V star (Förster Schreiber 2000). We therefore estimated the spectral type (and $T_{\rm eff}$) of our targets by comparing their spectral energy distribution to the L00 and KH86 dwarfs, and tested this estimate using the equivalent width of the NaI $\lambda 2.21\mu$ absorption line in the I04 spectra.

For the comparison of the SED, we first shifted our data to the rest wavelength of the NaI $\lambda 2.21\mu$ line, then smoothed our and KH86's data to match the resolution of the L00 data, and finally normalised all three data sets by dividing through the average flux value of the 2.10–$2.14\,\mu$ wavelength interval. The results of the visual comparison are summarised in Table 3. This, and the subsequent analysis, does not include the object NN Ser, since the S/N proved too low for the detection of absorption features. For completeness, we present its unsmoothed spectrum in Fig. 1.

Such visual comparison over a limited spectral range can certainly yield only a very rough estimate of the spectral type. Since several members of our sample have been found to show significant irradiation by the white dwarf, one should furthermore expect that those stars appear somewhat bluer, and that the corresponding temperatures will be overestimated.

We can test these estimates by measuring the strength of suitable absorption features in our spectra. In the *K* band, the NaI $\lambda 2.21\mu$ line appears as the best choice, since it shows a distinctive dependence of temperature, but is independent of luminosity class, and thus nuclear evolution (Ivanov et al. 2004, their Fig. 9). The stars in the I04 library were taken with the same instrumentation as our targets, although at a slightly lower spectral resolution, and we smoothed our spectra correspondingly. We then normalised the spectra for their SED by fitting splines to the continuum and dividing by the fit. These spectra are shown in Fig. 2. Equivalent widths were measured using the index definition from Ali et al. (1995) as listed in I04. The results are summarised in Table 3 and plotted in Fig. 3, together with the stars from the I04 catalogue.

Table 3. Estimated spectral type and corresponding effective temperature of the targets based on their SED. For comparison, the spectral types from the literature (listed in Table 1) are repeated here (in brackets). The error in the temperature column corresponds to the estimated range. The last column gives the equivalent width (in Å) of the NaI $\lambda 2.21\,\mu$ absorption line. The table is sorted with respect to the strength of the latter.

object	spType	$\log T_{\rm eff}$	NaI
RR Cae	M3–M4.5 (≳M6V)	3.510(10)	3.4
UZ Sex	M2.5–M5 (M4V)	3.515(25)	3.5
EC 13349-3237	K2–M1	3.590(60)	3.9
RE 1016-053	K1–K5 (M1.5V)	3.670(30)	4.1
BPM 71214	K2–M1 (M2.5V)	3.590(60)	4.9
LTT 560	M5.5–M6 (M5.5V)	3.430(20)	4.9
EC 13471-1258	M3.5–M5 (M3.5–M4V)	3.485(25)	5.2
BPM 6502	M2.5–M5	3.500(40)	5.6
EC 12477-1738	M3.5–M5	3.475(15)	6.0
P83l-57	M2.5–M3.5	3.510(30)	6.4
CC Cet	M3.5–M5.5 (M4.5–M5V)	3.480(30)	7.8
EC 14329-1625	M3.5–M4.5	3.495(15)	8.1
LP 759-25	M5.5–M6 (M5.5V)	3.430(20)	4.3
J223315.83-603224.0	M1–M2.5 (M2V)	3.530(10)	4.6
1E 2310.4-4949	M3–M4.5 (M3Ve)	3.485(25)	5.2

Although this index presents a large scatter even within the library stars, the plot does show that the pre-CVs on the average appear to have slightly higher equivalent widths at a given temperature. With CC Cet and EC 14329-1625 there are two systems with exceptionally strong NaI absorption, be it due to enhanced NaI, or due to a much later spectral type than estimated (note, however, that our estimate for CC Cet fits well the result from Saffer et al. 1993). On the other hand the two confirmed M5.5-M6 dwarfs LTT 560 and LP 759-25 (the latter being one of the comparison stars) have a comparatively shallow NaI absorption line. Still, on the whole, our estimates appear consistent with the behaviour of the NaI spectral index.

The referee suggested to use the 2MASS *JHK* database in order to further explore the possibility that irradiation by the primary alters the intrinsic SED in the *K* band, thus causing an overestimation of the temperature in our targets. In Fig. 4, we present the corresponding colour-colour diagram to compare our targets with the late-type dwarfs from the spectroscopic catalogues of Ali et al. (1995), Kleinmann & Hall (1986), Ivanov et al. (2004), and Leggett et al. (2000). Following Hoard et al. (2002), we have also included the main-sequence from Cox (2000, p.151), converted to the 2MASS photometric system using the transformations from Carpenter (2001). Irradiation would make the secondary stars in pre-CVs appear bluer, and thus result into a displacement towards the lower left of the main sequence. We do find four of our targets in this direction, but still well within the general scatter that is observed also for single late-type stars. Three targets lie somewhat above the main-sequence, i.e. they show an excess in their *H* magnitude, the most extreme case being EC 13349-3237. A second system worth mentioning is LTT 560. As we discuss in Sect. 4.2, its *K* band spectrum is very similar to the M5.5 dwarf LP 759-25. The near-infrared colours of the two stars, however, do not match, with LTT 560 being distinctively bluer (Table 1), and it appears in Fig. 4 as a blueshifted M4 dwarf. Still, this system contains a very cool white-dwarf primary ($T_{\rm WD} \sim 7500$ K, Tappert et al. 2007), and this displacement can therefore not be due to irradiation. Note also that the primary of RR Cae has a very similar temperature, and since this object does not appear blueshifted, it is unlikely that
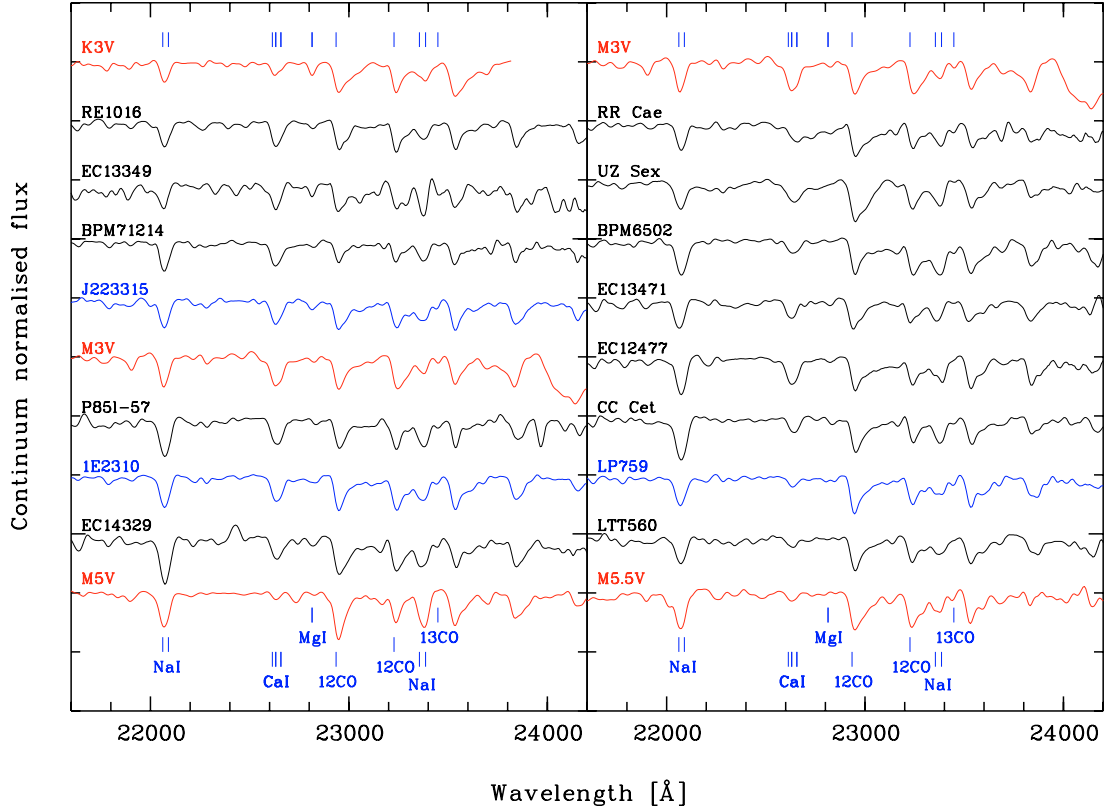
Fig. 2. Continuum-normalised target spectra. The data have been smoothed to match the resolution of Ivanov et al. (2004). Spectra are roughly sorted according to their estimated spectral type. For comparison, the plot also includes the following objects from Ivanov et al.: HR8832 (K3V), GJ388 (M3V), GJ866 (M5V), and GJ905 (M5.5V).
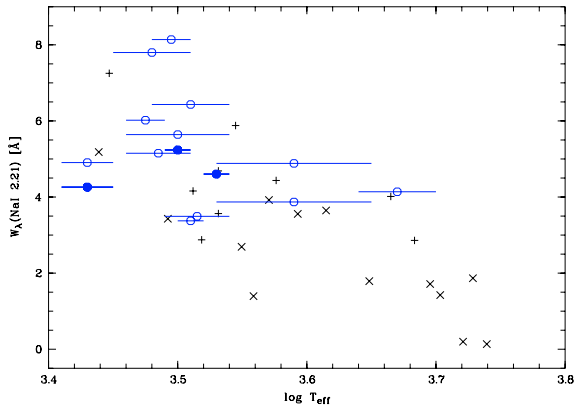

Fig. 3. Equivalent width of NaI as a function of effective temperature. Stars from Ivanov et al. (2004) with $-0.1 \leq$ [Fe/H] ≤ 0.1 are marked by $+$, those with metallicities outside this range, or, in the one case of the star with the lowest $T_{\rm eff}$, unknown, with $\times$. Open circles indicate the pre-CVs from our sample, filled ones represent the three comparison late-type dwarfs.

Fig. 4. Colour–colour diagram of the 2MASS $JHK_{\rm s}$ photometry. The plot includes late-type dwarfs from spectroscopic libraries (crosses), main-sequence colours (filled circles), and pre-CVs (open circles). The latter are labelled in sequence of increasing $H - K_{\rm s}$ as follows: (1) EC 13349-3237, (2) P83l-57, (3) RE 1016-053, (4) BPM 71214, (5) CC Cet, (6) EC 12477-1738, (7) LTT 560, (8) UZ Sex, (9) EC 13471-1258 (10) EC 14329-1625, (11) RR Cae, (12) BPM 6502. Only systems with photometric errors <0.05 in either of the colours are shown. The cross in the upper left corner indicates the average error ~0.036 mag for the objects included in this plot.

contribution from the white dwarf itself is causing this shift in LTT 560. Photometric light curves show evidence for flaring activity, and so the displacement might be explained by 2MASS having caught LTT 560 during an active phase.

In Table 4 we compare the spectral types of our targets determined with the three different methods. If irradiation had any effect on the *K*-band SED, we would expect that the spectral-type estimates from 2MASS and from SED agree well with each other, but not with the estimates from the line strengths. The fact that we find all three methods providing very similar results (± 1 subclass) for most of the systems shows that this is not the case.
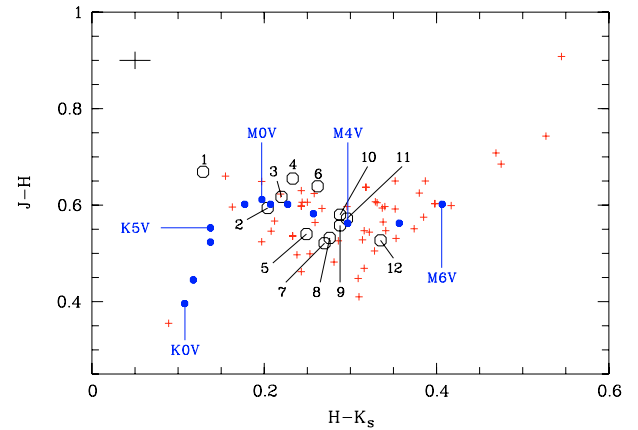
4.2. The ^{12}CO absorption

The principal result of the *K*-band spectroscopy of cataclysmic variables by Harrison et al. (2004, 2005a,b) was the unusual weakness of the ^{12}CO absorption together with enhanced ^{13}CO.
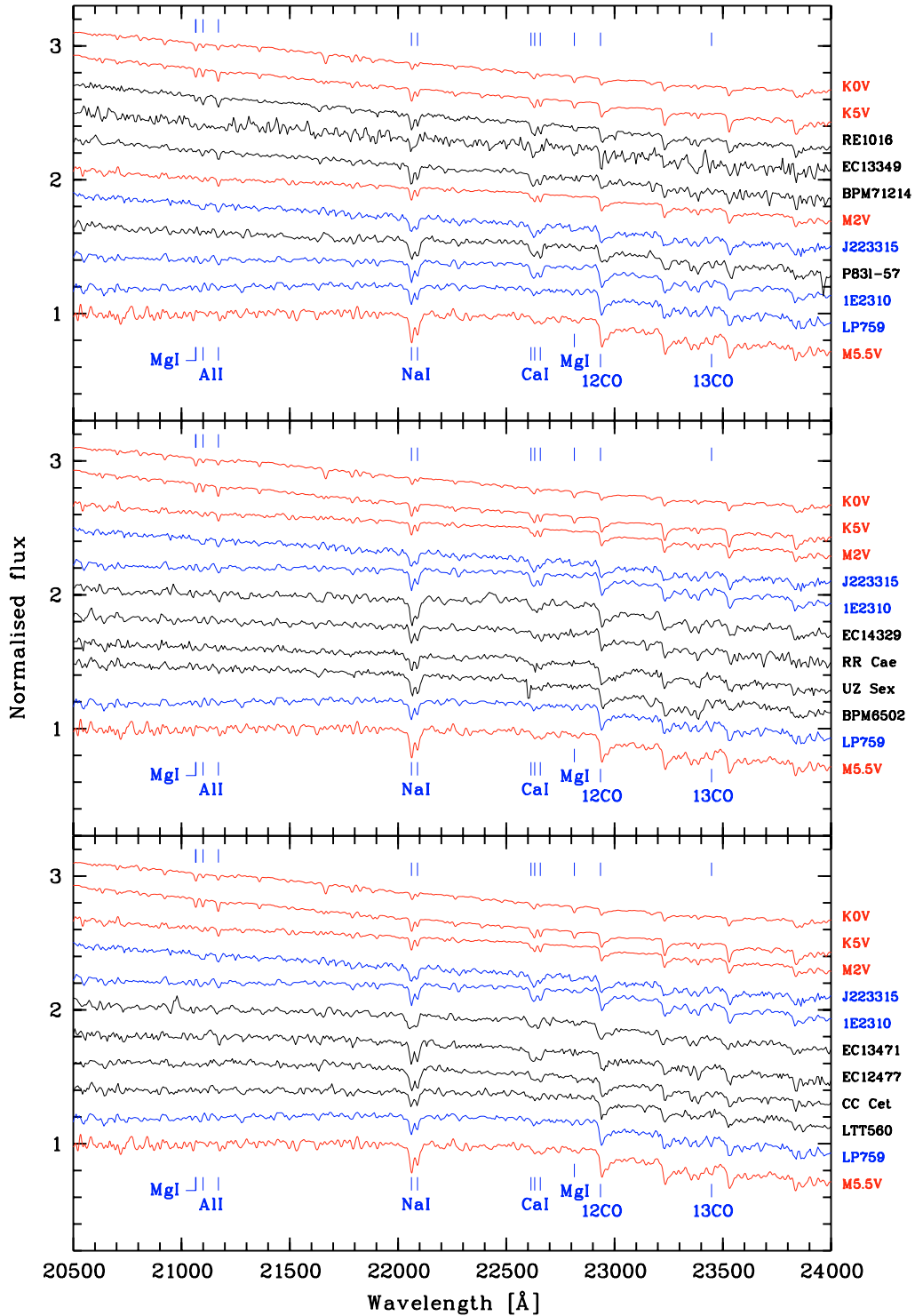
Fig. 5. Unsmoothed, normalised spectra. Each plot includes four pre-CVs, the three comparison stars, and the four late-type dwarfs from the Kleinmann & Hall (1986) catalogue. The individual spectra are vertically displaced by 0.2 units. The sequence roughly corresponds to the estimated spectral type, with the plot at the top containing the earliest, and the one at the bottom the latest. Note that the M2V standard, Gl 411, has a rather low metallicity of −0.33 dex (Bonfils et al. 2005), resulting in generally weaker absorption features.

While a more quantitative method would in principle be desirable, we here follow the approach by Harrison et al. and visually compare our target spectra to single stars of similar spectral type. The reason for this is that the only available library that includes a large number of late-type dwarfs at sufficient spectral resolution by Ivanov et al. (2004) contains continuum normalised data. For the comparison of the NaI absorption, this did not pose a great difficulty, since the blue part can be fitted relatively easily. Furthermore, the slope of the NaI relation with temperature is steep, making the NaI strength a comparatively robust parameter. In contrast, in the red part of the spectrum, the continuum is not well defined due to the extended and overlapping CO absorption bands. Systematic differences between the library stars

Table 4. Comparison of the spectral types estimated via the 2MASS colour–colour diagram, the *K* band spectral energy distribution, and the line strengths in the *K* spectra. The last column gives previous estimates from the literature (for references see Table 1). Systems that lie above or below the main-sequence in the two-colour diagram are marked by "+*H*" and "+blue", respectively.

object	*JHK*	SED	lines	literature
BPM 6502	M4–M5 +blue	M2.5–M5	M5	–
BPM 71214	M2 +*H*	K2–M1	M3	M2.5
CC Cet	M3.5 +blue	M3.5–M5.5	M3–M5.5	M4.5–M5
EC 12477	M3 +*H*	M3.5–M5	M3	–
EC 13349	>K5 +*H*	K2–M1	K5–M2	–
EC 13471	M4	M3.5–M5	M2	M3.5–M4
EC 14329	M4	M3.5–M4.5	M3	–
LTT 560	M4 +blue	M5.5–M6	M5.5	M5.5
P83l-57	M1	M2.5–M3.5	M3	–
RE 1016	M1.5	K1–K5	K5–M2	M1.5
RR Cae	M4	M3–M4.5	M4	≳M6 / M4
UZ Sex	M4 +blue	M2.5–M5	M4	M4

and our data are thus easily introduced right in the spectral range that is of most interest.

We therefore turn to the aforementioned visual approach and in Fig. 5 present a comparison of our unsmoothed spectra with the KH86 data. For this purpose, the latter have been smoothed to match our spectral resolution. In the following we summarise the results for each object in detail.

BPM 6502: This object was observed twice, unfortunately both times with unsatisfactory results. The first spectrum showed a strong deviation of the SED in the blue part of the spectral range, while a broad 'emission' feature affected the red part (2.27–2.35 μ). We attempted to remove the latter by fitting a broad Gaussian, and this spectrum is shown in Fig. 5 (middle plot). There remained, however, notable differences in comparison with the – apparently unaffected – red part of the first spectrum, so the latter was used to measure equivalent widths (and is presented in Fig. 2).

There is no previous estimate on the spectral type of the secondary in this system, but Kawka et al. (2000) find a mass to $M_2 = 0.16(09) M_\odot$, indicative of an ~M5-M6 dwarf. The *K*-band SED points to a somewhat earlier type. However, as explained above, that SED is not entirely trustworthy. Indeed, the NaI and CaI line strengths suggest a spectral type close to M5V, since they are similar to the M5.5V standard from KH86 (NaI is a bit weaker, and CaI slightly stronger). All CO absorption bands show normal strengths.

BPM 71214: Kawka et al. (2002) give M2.5V as spectral type. Again, our SED analysis yields an earlier type, but the line strengths (NaI, CaI) are very similar to the M3Ve star 1E2310.4-4949, favouring the Kawka et al. result. This is supported by the weakness of the MgI $\lambda 2.11/2.28 \mu$ lines, which are barely, if at all, detected. On the other hand, the CO features are very weak for such spectral type and fit much better the K5V star from KH86.

CC Cet: This object was also observed twice. Both spectra were of sufficient quality, so that they could be combined in order to increase the S/N. The spectral type suggested by the SED agrees well with the previous estimate of M4.5–M5 by Saffer et al. (1993). Also the line strengths place the object between the M3Ve star 1E2310.4-4949 and KH86's M5.5 dwarf. In comparison, the CO absorption appears slightly too weak.

EC 12477-1738: The spectroscopic characteristics are similar to CC Cet. The stronger CaI indicates a slightly earlier type, probably closer to M3V than M5.5V. CO appears at about the same strength as in CC Cet.

EC 13349-3237: The faintest member of our sample (apart from NN Ser), and this is unfortunately reflected in the low S/N. SED and line strengths both place it somewhere between the KH86's K5V and M2V, with the clearly detected MgI $\lambda 2.28 \mu$ line pointing to the earlier limit of this range. Worth noting is furthermore the non-detection of the AlI $\lambda 2.11/2.12 \mu$ lines. These have lesser strength than MgI only for spectral types earlier than K5V. In contrast, CO bands are clearly visible, although the low S/N impedes a more precise comparison of their strength.

EC 13471-1258: O'Donoghue et al. (2003) found that this system is already close to start its CV phase, and estimated its spectral type to M3.5–M4V. The absorption features in our spectrum, comparatively weak NaI, CaI, and CO, place it close to the M2V star J223315.83-603224.0, although both the 2MASS colours and the *K*-band SED agree better with the former estimate.

EC 14329-1625: The spectrum shows great similarities with the M3Ve star 1E2310.4-4949, with the notable exception of the enhanced NaI line.

LTT 560: This object is almost a spectroscopic twin to the M5.5 dwarf LP 759-25, with only slightly weaker absorption lines and bands. LTT 560 is a remarkable system in many aspects: it contains the coolest white dwarf in a pre-CV besides RR Cae, and there is evidence for stellar activity and low-level mass transfer, although the secondary star does not fill its Roche lobe (Tappert et al. 2007). Its *K*-band spectrum, however, does not show any anomalies.

P83l-57: NaI and CaI line strengths are similar to the M3Ve star 1E2310.4-4949, while the CO bands resemble more those in the M2 dwarf J223315.83-603224.0. Initial suspicions about photometric variability in the form of a sinusoidal or ellipsoidal light curve (Tappert et al. 2004) could not be confirmed. Since there are a several narrow emission lines detected in the optical spectrum (e.g., Ca H and K, and the Balmer series; Rodgers & Roberts 1994), this object is either a wide, detached, binary with a very active red dwarf, or – somewhat more likely – seen at low orbital inclination. Note also that the 2MASS data indicates a slightly earlier type (M1V) which could be due to irradiation, implying that this system indeed has a hot companion.

RE 1016-053: Both SED and the NaI and CaI are very similar to BPM 71214, although the presence of the MgI lines indicates an earlier type. Comparison with the KH86 stars on the basis of the MgI strength with respect to AlI places the star somewhat later than K5V and somewhat earlier than M2V, in good agreement with Thorstensen et al. (1996), who found M1.5V. The CO bands appear at normal strength, and stronger than in BPM 71214, emphasising their weakness in the latter star.

RR Cae: The SED of this star fits best with the M3.5V standards from the L01 library. Bruch & Diaz (1998) find ≳M6V, but this appears unlikely, since the blue part of the spectrum does not show any evidence of the H_2O depression that is typical for late M dwarfs. RR Cae contains a very cool white dwarf primary ($T_{WD} \sim 7000$ K; Bragaglia et al. 1995), so that there are no irradiation effects present that could alter the intrinsic slope of the secondary's continuum. Both SED and line strengths are similar to UZ Sex, which has been classified as M4V (Saffer et al. 1993). Furthermore, a recent study on optical spectra of RR Cae by Maxted et al. (2007) also finds an M4V secondary star, in

good agreement with our infrared data. For such spectral type, the CO bands show normal abundances.

UZ Sex: As mentioned above, this is probably an M4V star with perfectly normal abundances.

We close this section with the remark that, while we detect ^{13}CO in all stars in our sample, none of the systems shows it at anomalous strength.

5. Discussion and conclusion

With BPM 71214 we find one system in our sample that at first glance appears as a promising candidate for diminished ^{12}CO. There seem to be certain problems with the reduction for telluric features, as indicated by two unexplained absorption lines at 2.318 μ and 2.372 μ (Fig. 5). However, if additional telluric absorption should also affect the CO band, this would result in enhanced absorption, and not in the observed diminished one. In any case, this potential depletion of CO is not nearly as dramatic as found in certain CVs (Harrison et al. 2004, 2005b). Taking into account the spread of CO line strengths in single late-type dwarfs (Ivanov et al. 2004, their Fig. 9), and also the fact that none of our systems shows any enhancement of ^{13}CO with respect to ^{12}CO, we conclude that, at least regarding the CO abundance, all pre-CVs in our sample are consistent with main-sequence stars.

A comparatively large fraction of our targets appears to have abnormally strong NaI absorption (Fig. 3, Table 3). While in three systems (RE 1016−053, BPM 71214, P83l−57) such potential enhancement is unclear due to the uncertainty regarding their spectral type, both CC Cet and especially EC 14329−1625 inhabit a stronger NaI line than any other star in the Ali et al. (1995), Ivanov et al. (2004), and Kleinmann & Hall (1986) catalogues. All these catalogues only include M dwarfs up to ∼M5.5, but Cushing et al. (2005) have shown that NaI has maximum strength at ∼M6V and diminishes towards later spectral types, disappearing completely around ∼L1. The enhanced line in CC Cet and EC 14329−1625 is therefore not due to an erroneous assignation of the spectral type. However, since the uncertainties in the spectral type for the three above mentioned systems are comparatively large, and since the effect in CC Cet is not overly dramatic (Cushing et al. 2005 give $W_{\lambda,\mathrm{NaI}} = 7.6 \pm 0.2$ Å for the M6V star Gl 406, while CC Cet has $W_{\lambda,\mathrm{NaI}} = 7.8$ Å), it is well possible that this apparent anomaly of a group of pre-CVs melts down to just one peculiar object, EC 14329−1625.

In agreement with previous results, most pre-CV secondary stars in our sample turned out to have spectral types ≳M2V, and therefore will not evolve within Hubble time (e.g. Pols et al. 1998). As discussed in Sect. 2, we therefore did not expect to be able to confirm scenario 1 (nuclear evolution of the secondary star). The possibility that processed material is accreted by the secondary star during the CE phase has been investigated in detail by Marks & Sarna (1998), who find that such potential accretion not can account for the abundance anomalies observed in CVs, since the accreted material will be stripped from the secondary star during the initial stages of mass-transfer. Our *K*-band spectra of pre-CVs now show that only a very small amount of CE material, if any, is accreted by the secondary, since it leaves no trace already in comparatively young pre-CVs.

There remain therefore two possibilities for the presence of anomalous CO strengths in certain CVs. Either these systems originate from a very different type of pre-CV (e.g., supersoft binaries; Schenker et al. 2002), or the material was accreted during nova eruptions.

Assuming for a moment the former, we point out that Harrison et al. (2005a) find that magnetic CVs have normal abundances, motivating them to suggest different formation mechanisms for magnetic and non-magnetic CVs. We here draw attention to the fact that there is no indication for any strong magnetic white dwarf primary in the systems of our sample (and they appear to be pretty rare in pre-CVs in general; Liebert et al. 2005; Silvestri et al. 2007). These objects therefore will eventually evolve into non-magnetic CVs without anomalous abundances. This does not invalidate the argumentation by Harrison et al. (2005a), but indicates that the evolution of CVs might even come in more flavours than hitherto suspected.

Our study furthermore emphasises the need for more data, both with respect to single late-type dwarfs in order to better address the abundance scatter within a specific spectral type, and regarding the large discrepancy between the number of known pre-CVs and CVs (e.g., Morales-Rueda et al. 2005; Ritter & Kolb 2003). Thanks to the Sloan Digital Sky Survey, the latter picture is improving tremendously (Silvestri et al. 2006, 2007). However, even this much enlarged sample of pre-CVs is still strongly biased towards 'young' pre-CVs and late-type secondary stars (Schreiber & Gänsicke 2003; Schreiber et al. 2006), and further studies will be necessary in order to establish a representative sample of CV progenitors.

References

Ali, B., Carr, J. S., Depoy, D. L., Frogel, J. A., & Sellgren, K. 1995, AJ, 110, 2415
Beuermann, K., Baraffe, I., Kolb, U., & Weichhold, M. 1998, A&A, 339, 518
Bonfils, X., Delfosse, X., Udry, S., et al. 2005, A&A, 442, 635
Bragaglia, A., Renzini, A., & Bergeron, P. 1995, ApJ, 443, 735
Bruch, A. 1999, AJ, 117, 3031
Bruch, A., & Diaz, M. P. 1998, AJ, 116, 908
Carpenter, J. M. 2001, AJ, 121, 2851
Cox, A. N. 2000, Allen's astrophysical quantities, 4th Ed. (New York: AIP Press; Springer)
Cushing, M. C., Rayner, J. T., & Vacca, W. D. 2005, ApJ, 623, 1115
Downes, R. A., Webbink, R. F., Shara, M. M., et al. 2005, J. Astron. Data, 11, 2
Förster Schreiber, N. M. 2000, AJ, 120, 2089
Gänsicke, B. T. 2005, in The Astrophysics of Cataclysmic Variables and Related Objects, ed. J.-M. Hameury, & J.-P. Lasota, ASP Conf. Ser., 330, 3
Gänsicke, B. T., Szkody, P., de Martino, D., et al. 2003, ApJ, 594, 443
Haefner, R. 1989, A&A, 213, L15
Haefner, R., Fiedler, A., Butler, K., & Barwig, H. 2004, A&A, 428, 181
Harrison, T. E., Osborne, H. L., & Howell, S. B. 2004, AJ, 127, 3493
Harrison, T. E., Howell, S. B., Szkody, P., & Cordova, F. A. 2005a, ApJ, 632, L123
Harrison, T. E., Osborne, H. L., & Howell, S. B. 2005b, AJ, 129, 2400
Hellier, C. 2001, Cataclysmic Variable Stars (Springer)
Hoard, D. W., & Wachter, S. 1998, PASP, 110, 906
Hoard, D. W., Wachter, S., Clark, L. L., & Bowers, T. P. 2002, ApJ, 565, 511
Ivanov, V. D., Rieke, M. J., Engelbracht, C. W., et al. 2004, ApJS, 151, 387
Kawka, A., Vennes, S., Dupuis, J., & Koch, R. 2000, AJ, 120, 3250
Kawka, A., Vennes, S., Koch, R., & Williams, A. 2002, AJ, 124, 2853

Kilkenny, D., O'Donoghue, D., Koen, C., Stobie, R. S., & Chen, A. 1997, MNRAS, 287, 867

Kirkpatrick, J. D., Henry, T. J., & Simons, D. A. 1995, AJ, 109, 797

Kleinmann, S. G., & Hall, D. N. B. 1986, ApJS, 62, 501

Kube, J., Gänsicke, B. T., & Hoffmann, B. 2002, in The Physics of Cataclysmic Variables and Related Objects, ed. B. T. Gänsicke, K. Beuermann, & K. Reinsch, ASP Conf. Ser., 261, 678

Leggett, S. K., Allard, F., Dahn, C., et al. 2000, ApJ, 535, 965

Liebert, J., Wickramsinghe, D. T., Schmidt, G. D., et al. 2005, AJ, 129, 2376

Marks, P. B., & Sarna, M. J. 1998, MNRAS, 301, 699

Maxted, P. F. L., O'Donoghue, D., Morales-Rueda, L., Napiwotzki, R., & Smalley, B. 2007, MNRAS, 376, 919

Morales-Rueda, L., Marsh, T. R., Maxted, P. F. L., et al. 2005, MNRAS, 359, 648

O'Donoghue, D., Koen, C., Kilkenny, D., et al. 2003, MNRAS, 345, 506

Oliver, S., Mann, R. G., Carballo, R., et al. 2002, MNRAS, 332, 536

Patterson, J. 1998, PASP, 110, 1132

Pols, O. R., Schroder, K.-P., Hurley, J. R., Tout, C. A., & Eggleton, P. P. 1998, MNRAS, 298, 525

Ritter, H., & Kolb, U. 2003, A&A, 404, 301

Rodgers, A. W., & Roberts, W. H. 1994, IAU Circ., 6043, 2

Rousselot, P., Lidman, C., Cuby, J.-G., Moreels, G., & Monnet, G. 2000, A&A, 354, 1134

Saffer, R. A., Wade, R. A., Liebert, J., et al. 1993, AJ, 105, 1945

Schenker, K., & King, A. R. 2002, in The Physics of Cataclysmic Variables and Related Objects, ed. B. T. Gänsicke, K. Beuermann, & K. Reinsch, ASP Conf. Ser., 261, 242

Schenker, K., King, A. R., Kolb, U., Wynn, G. A., & Zhang, Z. 2002, MNRAS, 337, 1105

Schreiber, M. R., & Gänsicke, B. T. 2003, A&A, 406, 305

Schreiber, M. R., Nebot Gomez-Moran, A., & Schwope, A. D. 2006 [arXiv:astro-ph/0611461]

Silvestri, N. M., Hawley, S. L., West, A. A., et al. 2006, AJ, 131, 1674

Silvestri, N. M., Lemagie, M. P., Hawley, S. L., et al. 2007, AJ, in press [arXiv:0704.0789v1]

Stocke, J. T., Morris, S. L., Gioia, I. M., et al. 1991, ApJS, 76, 813

Tappert, C., Gänsicke, B. T., & Mennickent, R. E. 2004, in Rev. Mex. Astron. Astrofis. Conf. Ser., ed. G. Tovmassian, & E. Sion, 245

Tappert, C., Gänsicke, B. T., Mennickent, R. E., & Schmidtobreick, L. 2006a, Ap&SS, 304, 299

Tappert, C., Toledo, I., Gänsicke, B. T., & Mennickent, R. E. 2006b, in Rev. Mex. Astron. Astrofis. Conf. Ser., 177

Tappert, C., Gänsicke, B. T., Schmidtobreick, L., et al. 2007, A&A, submitted

Thorstensen, J. R., Vennes, S., & Bowyer, S. 1996, ApJ, 457, 390

Warner, B. 1995, Cataclysmic variable stars, Cambridge Astrophysics Series, (Cambridge, New York: Cambridge University Press)